

FULLY ONLINE CALIBRATION-COMPENSATION METHOD FOR ROTARY TABLE POSITIONING ERROR

Kairu Shao¹⁾, Weibin Zhu¹⁾, Yao Huang²⁾, Zi Xue²⁾, Jin Zhu³⁾

1) China Jiliang University, College of Metrology Measurement and Instrument, Hangzhou, 310018, China (✉ zhuweibin@cjlu.edu.cn)

2) National Institute of Metrology PR China, Beijing, 100029, China

3) Zhejiang Institute of Quality Sciences, Hangzhou, 310018, China

Abstract

Precision rotary table is an angular positioning generator commonly used in the industry. Ensuring its long-term stability of positioning accuracy is a key concern. Researchers have conducted extensive studies on the online calibration and real-time compensation of rotary table positioning errors. However, existing research often involves offline processing to some extent throughout the calibration and compensation stages. Currently, there is very little research on methods where the entire process of calibrating and compensating rotary table positioning errors is fully online. Therefore, this paper proposes a fully online calibration-compensation method for rotary table positioning errors, and develops a rotary table positioning error calibration-compensation system. Based on the Fourier self-calibration principle and the harmonic compensation principle, this method implements online calibration and real-time compensation of positioning errors using a heterogeneous processor. Throughout the entire process, data processing is guaranteed to be online. Experimental results show that the positioning accuracy of the rotary table improved from $[-150.0'', 137.9'']$ to $[-1.3'', 1.6'']$, effectively enhancing its precision. The proposed method is highly suitable for compact or cost-sensitive precision rotary tables, while also being applicable for spindle condition monitoring.

Keywords: precision rotary table, positioning error, online calibration, real-time compensation.

1. Introduction

Precision rotary tables are commonly used angular positioning generator, widely applied in CNC machine tools, angular metrology, aerospace, and other fields. These fields generally impose high requirements on rotary table positioning accuracy. However, the accuracy is often limited by factors such as mechanical structures, mechanical vibration, grating scale errors, and eccentric mounting of gratings. Concurrently, factors like load variation and degradation of mechanical structural performance cause the rotary table positioning error to change, necessitating regular calibration. However, it is a laborious and time-consuming process. Therefore, achieving the online calibration and real-time compensation for rotary table has become a key concern in industry.

The traditional methods for calibrating the rotary table positioning errors involve using polygon or a multi-tooth division table with a mirror combined with an autocollimator, or employing laser interferometers.[1] However, limited by the number of faces in polygon and the angular resolution of multi-tooth division table, the number of sample points is constrained, and the calibration procedure is relatively cumbersome, hindering automation. Consequently, metrologist have begun utilizing ring laser gyroscopes to calibration rotary tables.[2] Although ring laser gyroscopes offer ultra-high angular resolution and lower installation requirement, they suffer from issues like zero drift and temperature drift. Therefore, research on this method remains in its early stages.

The aforementioned methods all require auxiliary reference instruments for calibration. In contrast, self-calibration method can achieve calibration without reference instruments, attracting significant research attention, and various self-calibration methods have been proposed. Lu *et al.* proposed the *Time-measurement Dynamic reversal* (TDR) method based on rotary table's free-response model. This method calculates the free-response model parameters by measuring the pulse width of encoder signals using a high-frequency clock signal and derives the encoder error based on the circle closure principle and dynamic reversal [3, 4]. Wantanbe *et al.* introduced the *Equal-Division-Average* (EDA) method based on the harmonic characteristics of encoders [5]. It employs N read heads uniformly distributed around the grating disk; the sum of their measurement averaged yields the final evaluation result. This method can effectively require non-N-integer harmonic error components. While computationally simple, achieving higher accuracy with EDA method typically requires increasing the number of read heads. Although optimizing the arrangement of the read heads can reduce the required number while improving accuracy, this method still demands a relatively large number of read heads, imposing the higher cost requirement [6]. Ishii *et al.* proposed a *Virtual Equal Division Average* (VEDA) method [7]. Leveraging the harmonic characteristics of encoder periodic errors, it achieves the effect of multi-read heads EDA method using only two read heads. Similarly, based on the periodicity of encoder division errors, Geckeler *et al.* proposed a Fourier method based on transfer functions [8]. This methods require less read heads. Two or more read heads can achieve high-precision calibration. Furthermore, with more than four read heads, it can measure the radial error motion [9].

Error curve obtained by calibration typically needs to be compensated at the feedback end to improve the rotary table positioning accuracy. Wu *et al.* proposed a phase difference filtering method based on the harmonic characteristics of grating moiré fringe signals. By filtering out the second, third, and fourth harmonics of these signals, compensation is achieved [10]. Yang *et al.* proposed an error compensation method based on a *Radial Basis Function* (RBF) neural network, utilizing its strong local approximation capability for nonlinear mapping and fast learning speed to compensate for displacement [11]. Park *et al.* proposed a linear compensation method based on the mathematical model of encoder signals, improving various parameters through pre-calculation of offset, amplitude, and phase correction [12]. Zhao *et al.* achieved compensation for encoder eccentricity by adding several radial code tracks outside a traditional absolute encoder. Based on the physical model of encoder mounting eccentricity, this indirectly measures the eccentricity amount [13]. Zhao *et al.* proposed an encoder error compensation method using three calibration read heads and one measurement read head [14]. This method ensures the effective identification of the first ten harmonic components of the encoder's angular measurement error while requiring only a installation tolerance for the read heads. Zhou *et al.* proposed a real-time compensation method based on harmonic analysis [15]. It performs harmonic analysis on the calibrated encoder error curve and uses the *Coordinate Rotation Digital Computer* (CORDIC) algorithm for computation to achieve compensation. Gurauskis *et al.* employed polynomial fitting to compensate for geometric and temperature errors in linear encoders [16]. Comparison with finite element analysis results demonstrated the effectiveness of the polynomial fitting method. In the compensation methods mentioned above, data processing generally requires offline handling, and the compensation data is typically stored in the form of lookup tables in the controller's ROM, imposing certain requirements on the controller's storage capacity [17].

Although traditional cross-calibration methods are reliable, the requirement for auxiliary instruments alters the rotary table's load conditions, preventing the acquisition of positioning errors during its normal operating state. Among self-calibration methods, the TDR method relies on high rotary table rotation speeds, thus remaining primarily in the laboratory stage. While the Fourier method enables self-calibration of rotary table positioning errors and has

been applied in metrological standards, its data processing still currently depends on offline handling. The EDA method achieves real-time calibration and compensation and has been implemented in numerous devices [18–21]. However, limited by the number of read heads and its inherent principles, EDA exhibits significant suppression of specific low-order harmonics [22], preventing high accuracy in cost-sensitive or compact applications. Researchers have implemented real-time compensation through various approaches, such as harmonic fitting and polynomial fitting. Nevertheless, the acquisition and calculation of compensation parameters still rely on cross-calibration methods. To the best of our knowledge [23, 24], research on methods achieving further online processing of both rotary table positioning error calibration and compensation remains very scarce.

Therefore, this paper proposes a fully online calibration-compensation method for rotary table positioning errors, and develops a novel rotary table positioning error calibration-compensation system. Based on the Fourier self-calibration method, it utilizes dual read heads for online calibration. Leveraging the amplitude and phase information of the calibrated rotary table positioning error curve, it employs the CORDIC algorithm for harmonic calculation. This enables long-term online monitoring and compensation of rotary table positioning errors, thereby enhancing the positioning accuracy of cost-sensitive or compact rotary tables.

2. System principle

2.1. Principle of Fourier method using two read heads

According to ISO 230-1 [1], the rotary table positioning error $\varepsilon(\theta)$ can be defined as:

$$\varepsilon(\theta) = P(\theta) - \theta, \quad (1)$$

where $P(\theta)$ is the actual angular position of the turntable, and θ is the target position. Considering the circle closure principle, $\varepsilon(\theta)$ can be treated as a periodic function with a period of 2π . In practical applications, we assume two read heads are mounted on a common circle surrounding the grating disk, as shown in Fig. 1, with a subtended angle of α between them.

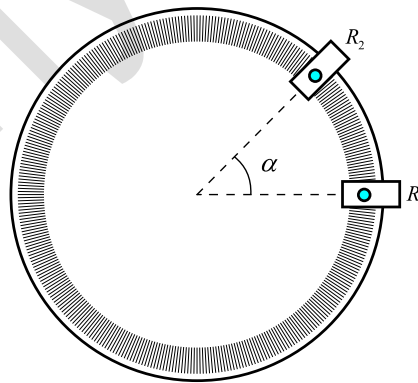


Fig. 1. The diagram of read head arrangement.

Assume the signal sampled by read head R_1 is:

$$R_1(\theta) = \theta + \varepsilon(\theta). \quad (2)$$

Therefore, the signal sampled by read head R_2 can be expressed by:

$$R_2(\theta) = \theta + \varepsilon(\theta + \alpha). \quad (3)$$

Subtracting these two signals yields:

$$\delta_{21}(\theta) = R_2(\theta) - R_1(\theta) = \varepsilon(\theta + \alpha) - \varepsilon(\theta). \quad (4)$$

Based on the properties of Fourier series, we obtain:

$$\delta_{21}(\theta) = \sum_{n=-\infty}^{+\infty} (e^{jn\alpha} - 1) E_n e^{jn\theta}, \quad (5)$$

where, E_n are the Fourier series coefficients of the rotary table positioning error curve $\varepsilon(\theta)$. Rearranging terms, the transfer function $TF(n)$ can be expressed as:

$$TF(n) = \begin{cases} \frac{1}{(e^{jn\alpha} - 1)}, & e^{jn\alpha} - 1 \neq 0 \\ 0, & otherwise \end{cases}. \quad (6)$$

Typically, we only analyze the first N harmonic components of the rotary table positioning error. Hence, the error curve $\varepsilon(\theta)$ can be represented as:

$$\varepsilon(\theta) = \sum_{n=-N}^N E_n e^{jn\theta} = \sum_{n=-N}^N D_{21}[n] TF(n) e^{jn\theta}, \quad (7)$$

where $D_{21}[n]$ is obtained by performing the Fourier transform on $\delta_{21}(\theta)$.

In the derivation above, we observe that the transfer function causes harmonic suppression, which affects the calibration accuracy of the Fourier method. The angular interval between read heads is the key variable controlling the transfer function's behavior. In our prior research, we conducted detailed analysis of this angular interval, yielding the following conclusions [25]: the angular separation should avoid circular division points where possible. If unavoidable, the angular separation at division points should be minimized. Meanwhile, smaller angular separation improves calibration accuracy but imposes tighter requirements on installation tolerance.

2.2. Principle of harmonic compensation

Utilizing the two-read-head Fourier method, the harmonic order information of the rotary table positioning error can be obtained. This information is used as a compensation value applied to the measured value through series summation. The calculation method is as follows:

$$\theta_{com}(\theta) = R(\theta) - \varepsilon(\theta) \approx R(\theta) - \varepsilon(R(\theta)), \quad (8)$$

where $R(\theta)$ is the measured value from the reference read head, and θ_{com} is the compensated measurement value of the rotary table. The rotary table positioning error $\varepsilon(\theta)$, obtained via the Fourier method, provides harmonic information in complex form. Using polar coordinates, it can be converted into a sum of cosine functions:

$$\varepsilon(\theta) = \sum_{n=-N}^N E_n e^{jn\theta} = a_0 + 2 \sum_{n=1}^N A_n \cos(n\theta + \Phi_n), \quad (9)$$

where $A_n = |E_n|$, $\Phi_n = \angle E_n = \tan^{-1} \frac{\text{Im}[E_n]}{\text{Re}[E_n]}$.

Common numerical methods for trigonometric functions include polynomial expansion and coordinate rotation. To meet the real-time requirements of error compensation, all calculations must be implemented in hardware circuitry. Therefore, this paper employs the CORDIC for trigonometric calculations. The CORDIC method iteratively approximates the target angle through vector rotation [26]. Its iterative calculation formulas are:

$$\begin{cases} x_{i+1} = x_i - y_i \cdot d_i \cdot 2^{-i} \\ y_{i+1} = y_i - x_i \cdot d_i \cdot 2^{-i} \\ z_{i+1} = z_i - d_i \tan^{-1}(2^{-i}) \end{cases}, \quad (10)$$

where $d_i = -1$, if $z_i < 0$; $+1$, otherwise. The initial conditions are:

$$\begin{cases} x_0 = \frac{1}{A_n} \\ y_0 = 0 \\ z_0 = \varphi \end{cases} \quad (11)$$

where $A_n = \prod_n \sqrt{1 + 2^{-2i}}$, then after n iterations, the result are:

$$x_n \approx \cos \varphi, y_n \approx \sin \varphi \quad (12)$$

In practical circuit implementations, the selection of iteration count and register bit-width affects the calculation accuracy of the CORDIC algorithm. Related discussions are provided in the appendices.

3. Design of the rotary table positioning error calibration-compensation system

To ensure the real-time performance of the rotary table positioning error calibration-compensation system, we selected the Xilinx XC7Z020CLG400-2 as the hardware platform [27]. It features 85k logic cells, 4.9 Mb of block RAM, and a dual-core ARM Cortex-A9 MPCore processor. A custom-designed FPGA circuit board is shown in Fig. 2. Based on the self-calibration principle of the two-read-head Fourier method and the harmonic compensation principle, a rotary table positioning error calibration-compensation system was designed using the custom FPGA board. The system block diagram is shown in Fig. 3.

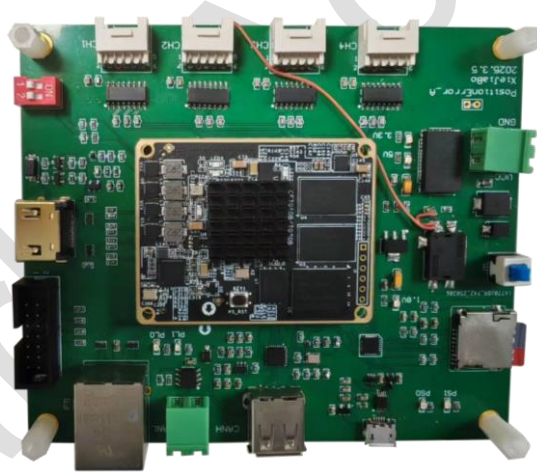


Fig. 2. Photograph of the custom-designed FPGA circuit board.

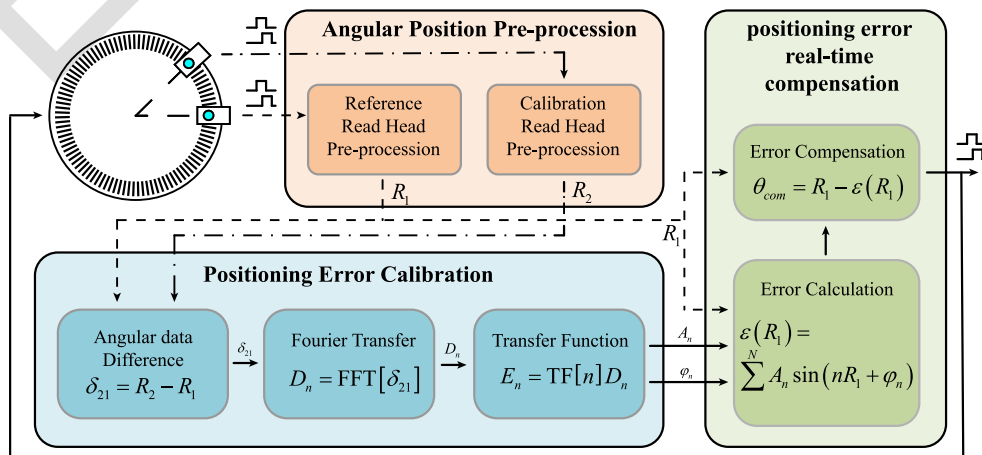


Fig. 3. The diagram of the rotary table positioning error calibration-compensation system.

As seen in Fig. 3, the system can be divided into three subsystems: the rotary table angular position pre-processing system, the rotary table positioning error self-calibration system, and the rotary table positioning error real-time compensation system. The rotary table is equipped with two read heads mounted at a fixed angular interval. One read head serves as the reference read head; its output measurement signal is used as the control feedback signal. After processing by the error compensation system, this signal connects to the rotary table servo feedback system. The other read head serves as the calibration read head and connects to the error calibration system. Its output measurement signal is used solely for calibration and does not directly participate in the rotary table's motion control. As established in section 2.1, the Fourier method requires prior knowledge of the angular interval between the two read heads. In our previous work, we identified this angular interval α - the sole variable in the transfer function as the critical parameter determining the calibration accuracy of the Fourier method. Based on conclusions from our prior research [25], we set the angular interval between the two read heads to 33° .

3.1. Design of rotary table angular position pre-procession system

To ensure real-time acquisition of angular data, the rotary table employs an incremental encoder. Through electronic interpolation, the read head outputs two quadrature square waves, as shown in Fig. 4.

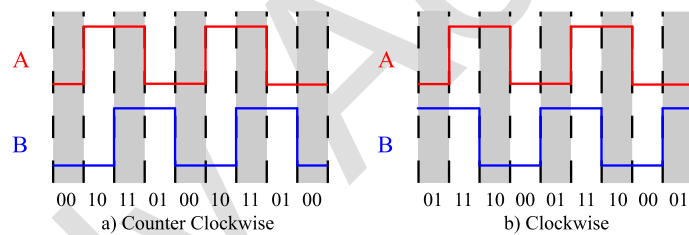


Fig. 4. The diagram of the square wave signal output from read heads.

Figure 4a shows the state of the two square wave signals during counter-clockwise rotary table rotation. Here, signal A leads signal B by 90° , and the level change sequence is 00, 10, 11, 01. Figure 4b shows the state during clockwise rotation. Here, signal A lags signal B by 90° , and the level change sequence is 00, 01, 11, 10. Based on this behavior, the relative angular motion of the rotary table is recorded by counting the edges of the two square waves. The direction of rotary table motion is determined by judging the phase relationship between the two signals. The rotary table's reference zero position is established by an index signal. Based on the logical relationship between these signals, the circuit structure for the rotary table signal pre-processing system was designed, as shown in Fig. 5.

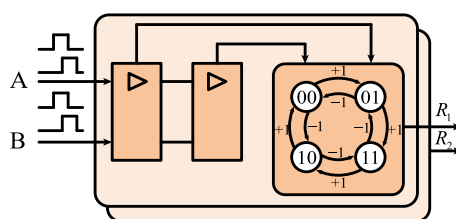


Fig. 5. The circuit structure of angular position pre-procession system.

As shown in Fig. 5, this circuit features two identical structures. They process the output signals from the two read heads in parallel and output the results to subsequent systems.

3.2. Design of rotary table positioning error self-calibration system

The rotary table positioning error self-calibration system internally generates a 1 kHz sampling clock. At the rising edge of each sampling clock, it latches the angular position values from the two read heads output by the pre-processing system and writes them into BRAM. As known from section 2.1, the self-calibration process using the Fourier method is complex. Implementing this calculation directly in circuitry would result in high complexity and significant development difficulty. However, leveraging the heterogeneous architecture of the ZYNQ platform, the calibration algorithm is executed on the CPU, ensuring circuit simplicity. After the rotary table completes one full rotation, the CPU reads the data measured by both read heads from the BRAM, performs calibration using the Fourier method, and subsequently updates the compensation parameters in the rotary table positioning error real-time compensation system via BRAM. This update transmits the calculated amplitude and phase information for each harmonic order. The circuit structure of this system is shown in Fig. 6.

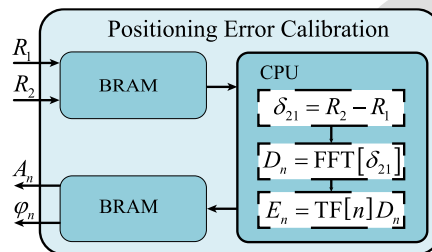


Fig. 6. The circuit structure of positioning error self-calibration system.

During the rotation of the rotary table, the circuit performs equidistant sampling, collecting 12000 data points per full rotation, with a sampling interval of approximately $108''$. Since the data length is divisible by the full circle, spectral leakage is effectively suppressed, thereby ensuring data reliability. Prior to calibration calculations, the data stored in BRAM must still be verified, primarily by checking whether the difference between adjacent sampling points is around $108''$.

Generally, rotary table positioning error changes are low-frequency and gradual, without sudden shifts. Therefore, we consider our calibration system to be real-time and online. Additionally, functionalities like human-computer interaction can be implemented on the CPU, enhancing the system's practicality.

3.3. Design of rotary table positioning error real-time compensation system

While ensuring real-time calibration of rotary table positioning errors, guaranteeing the rotary table's positioning accuracy critically depends on the real-time compensation of these errors. This aspect demands even higher real-time performance, requiring the compensation system to exhibit low latency and high processing speed. Therefore, we designed the rotary table positioning error real-time compensation system shown in Fig. 7.

As seen in Fig. 7, the real-time compensation system primarily consists of four computational units: the phase calculation unit, the harmonic calculation unit, the delay compensation unit, and the error compensation unit. The rotary table angular position pre-processing system inputs the value from the reference read head into the phase calculation unit. The phase calculation unit reads the updated phase information for each harmonic order from

the self-calibration system. Using multipliers, *lookup tables* (LUTs), and adders, it calculates the angle values for each harmonic order in parallel. The structure of this unit is shown in Fig. 8.

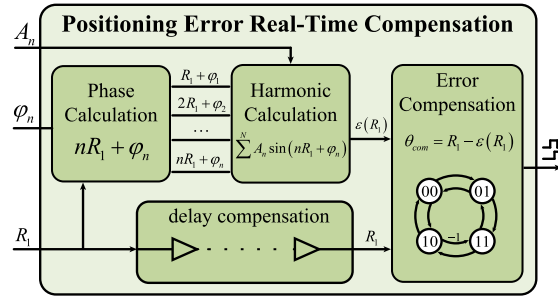


Fig. 7. The circuit structure of positioning error real-time compensation system.

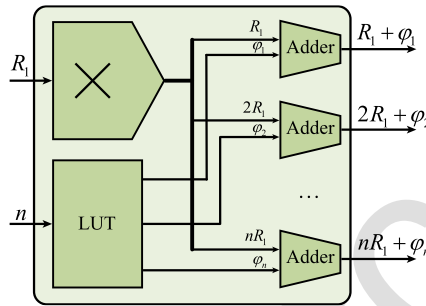


Fig. 8. The structure of the phase calculation unit.

The function of the harmonic calculation unit is to compute the values of each harmonic order based on the angle values provided by the phase calculation unit. Following the CORDIC trigonometric calculation principle mentioned in section 2.2, a pipelined architecture is designed as shown in Fig. 9. Utilizing simple shifters, adders, and LUTs, it obtains the cosine values for each harmonic order after 16 iterations. The selection of iteration count and register bit-width affects the calculation accuracy of the CORDIC algorithm. Related discussions are provided in the appendices.

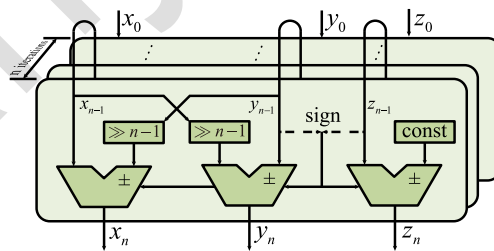


Fig. 9. The pipeline structure of CORDIC algorithm.

Since both the phase calculation unit and the harmonic calculation unit employ pipelined computation, a delay is introduced in the processing. This means that at any given moment, the harmonic value output by the harmonic calculation unit does not correspond to the angle value input at that same moment. Therefore, the delay compensation unit delays the input angle value. The duration of this delay matches the total computation time of the phase and harmonic calculation units. At this point (after the delay), the angle value output by the delay compensation unit and the harmonic value output by the harmonic calculation unit have a one-to-one correspondence. The delay compensation unit consists solely of multiple buffers.

The error compensation unit calculates the compensation value using the angle information from the delay compensation unit and the harmonic values from the harmonic calculation unit, according to (8). Finally, based on the relationship between the angle value and the signals shown in Fig. 5, it outputs the rotary table signal incorporating the compensation value.

Table 1. The delay amount of each unit in the real-time compensation system

Unit	Phase calculation unit	Harmonic calculation unit	Error compensation unit
Delay clock period	5	20	4
Delay time	50 ns	200 ns	40 ns

Table 1 summarizes the delay amount for each unit. As indicated in Table 1, the real-time compensation system introduces a final delay of 29 clock cycles. Considering the circuit clock frequency is 100 MHz, the system delay is 290 ns. This is far below the update frequency of the read head signals. Therefore, it can be considered that the real-time compensation system exhibits high real-time performance.

4. Experiment and discussion

This section presents the developed rotary table positioning error calibration-compensation system, as shown in **Błąd! Nie można odnaleźć źródła odwołania.**. In **Błąd! Nie można odnaleźć źródła odwołania.**a, the rotary table utilizes a MicroE PurePrecision grating disk and two M3000 read heads to provide angular position feedback signals. The grating disk has a diameter of 107.95 mm and features 16,384 grating lines over its entire circumference, corresponding to an approximate grating pitch of 20 μm . The two read heads are mounted around the grating disk at 33° interval with $\pm 50''$ installation tolerance, (considering the result in our previous work [25]). The angular installation interval and tolerances of the read heads are precisely determined and controlled through a purpose-built mechanical structure and tight machining tolerances. Each read head incorporates $1024 \times$ electronic interpolator, resulting in an overall rotary table angular resolution of $0.772''$. The rotary table motion controller (shown in **Błąd! Nie można odnaleźć źródła odwołania.**b) integrates components including a switching power supply, motor driver, and electronic display. It enables functionalities such as rotary table position control and human-machine interaction. The switching power supply provides DC power to the entire system. The motor driver employs an ACS SPiiPlus motion controller for rotary table motion control. Positioned adjacent to the rotary table motion controller in **Błąd! Nie można odnaleźć źródła odwołania.**b, the calibration-compensation system processes signals from the read heads and feeds back the processed signals to the rotary table motion controller. It utilizes a custom-designed circuit board (shown as **Błąd! Nie można odnaleźć źródła odwołania.**) incorporating the circuits described in section 3 for real-time compensation and feedback of the rotary table's angular position signals.

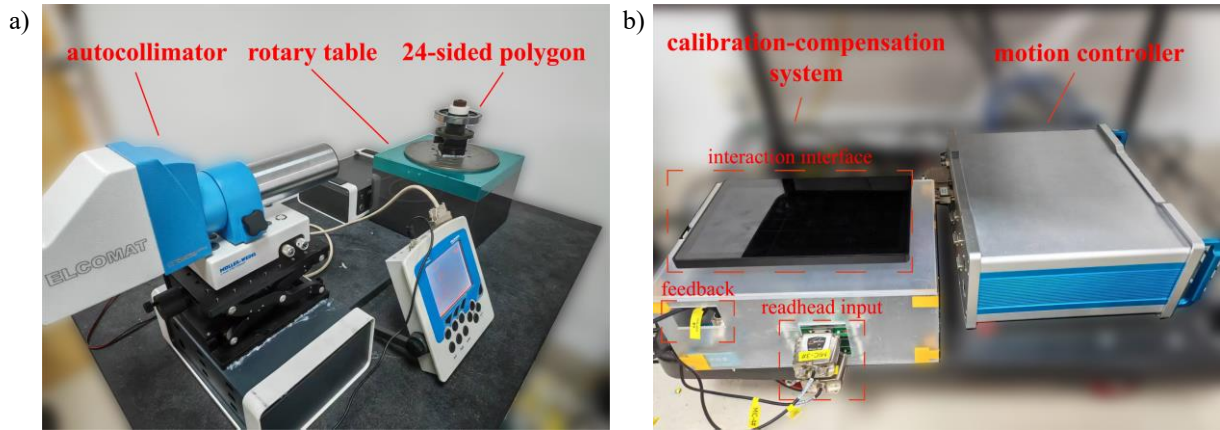


Fig. 10 The rotary table positioning error calibration-compensation system and experimental platform: a) rotary table with experimental facilities, b) calibration-compensation system and motion controller.

We used a 24-sided polygon and an autocollimator, which is ELCOMAT 3000, to measure the rotary table's positioning accuracy before and after activating the rotary table positioning error calibration compensation system, which is shown in Fig. 10a. Experiments were conducted in a temperature-controlled environment maintained at $20^{\circ}\text{C} \pm 2^{\circ}\text{C}$. The accuracy of the measuring equipment is as shown in Table 2.

Table 2. Specifications of the measuring equipment in experiment

Device	Model	Range	Uncertainty ($k = 2$)
Autocollimator	ELCOMAT3000	$\pm 1000''$	$\pm 0.1''$
Polygon	24-sided polygon	$0^{\circ} \sim 360^{\circ}$	$\pm 0.2''$

First, we measured the rotary table positioning accuracy without compensation by the calibration-compensation system. Subsequently, we activated the system's online calibration-compensation function and remeasured the positioning accuracy. Each measurement comprised sampling points equal to the number of polygon faces. Both scenarios underwent ten measurement cycles to evaluate the positioning repeatability of the rotary table system. The final results are shown in **Błąd! Nie można odnaleźć źródła odwołania.**, where the red curve represents the rotary table positioning error without the proposed compensation system, and the blue curve shows the error after compensation.

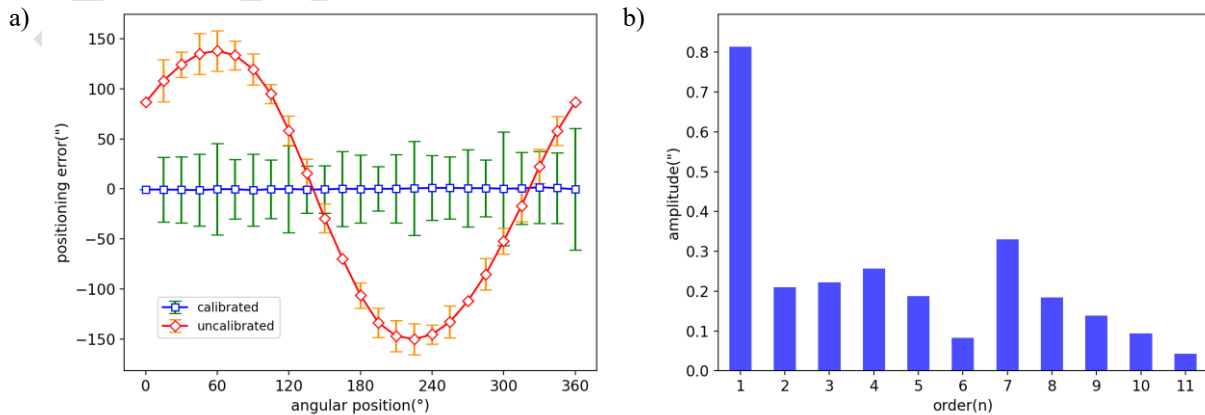


Fig. 11 Measurement results of autocollimator and polygon (a) (Standard Deviation $300 \times$ Scale Factor) and (b) harmonic analysis of measurement result of autocollimator and polygon.

Repeatability at 24 measurement points is expressed by the standard deviation of single measurements. The standard deviation estimate is given by Bessel's formula:

$$\sigma = \sqrt{\frac{\sum(x_i - \bar{x})^2}{n-1}}, \quad (13)$$

Where x_i denotes measured values, \bar{x} their mean, and n the number of measurements ($n = 10$ in this experiment). The standard deviation of ten repeated measurements at each angular position was evaluated using this formula and displayed with $300\times$ visual scaling in Fig. 11a. Figure 11a indicates that the maximum standard deviation does not exceed $0.2''$, residing within one order of magnitude of the rotary table's minimum resolution. Thus, the angular position errors obtained from ten measurements exhibit consistently high reliability.

Figure 11 demonstrates that after compensation by the proposed system, rotary table positioning accuracy improved from $[-150.0'', 137.9'']$ to $[-1.3'', 1.6'']$. The harmonic analysis of residual positioning error (Fig. 11b) shows no distinct harmonic characteristics overall, although the first-order harmonic remains relatively high compared to the others - likely due to installation eccentricity of the polygon. Apart from this, the remaining harmonics exhibit no clear pattern, indicating that random errors serve as the primary residual source. This confirms effective compensation of most positioning error components. The system successfully enables online calibration and compensation of rotary table positioning errors, significantly enhancing accuracy. Measurement uncertainty may also contribute to residual errors; its analysis follows.

In the experimental platform, uncertainty sources include: polyhedron measurement errors, autocollimator measurement errors, measurement repeatability errors, polyhedron mounting eccentricity, and polyhedron tower difference. These uncertainty components are summarized in Table 3. The calculated expanded uncertainty U is $0.46''$, one order of magnitude smaller than the residual positioning error post-compensation. This verifies the reliability of experimental results and conclusions.

Table 3. Summary of measurement uncertainty

No.	Sources of uncertainty	Symbol	Type of assessment	Standard uncertainty (")
1	Polyhedron measurement error	u_1	B	0.1
2	Autocollimator measurement error	u_2	B	0.05
3	Measurement repeatability error	u_3	A	0.2
4	Polyhedron mounting eccentricity	u_4	A	0.0005
5	Polyhedron tower difference	u_5	A	0.0001
Combined standard uncertainty $u = 0.23''$				
Expanded measurement uncertainty $U = 0.46''$				

The standard measurement uncertainty caused by polyhedron measurement errors and autocollimator measurement errors is provided by the metrology institution, with values of $0.1''$ and $0.05''$ respectively. The standard measurement uncertainty from measurement repeatability equals the mean variance of angular position errors calculated using Bessel's formula, resulting in $0.2''$. Uncertainty induced by mounting eccentricity of the polygonal mirror depends on surface flatness and reflector size, calculated as [28]:

$$u_4 = \frac{8sh}{H^2} \rho, \quad (14)$$

where s represents mounting eccentricity distance, h denotes surface flatness error, H is reflector width, and ρ is the radian-to-arcsecond conversion constant 206265. In the

experimental setup, we controlled $s \leq 1\mu\text{m}$. With $h = 0.03\mu\text{m}$ and $H = 10\text{mm}$, the resulting standard uncertainty $u_4 = 0.0005''$.

Tower difference refers to installation tilt of the polygonal mirror. Its induced uncertainty is [28]:

$$u_5 = \sin \alpha \frac{\sin^2 \tau}{\cos \tau} \rho, \quad (15)$$

where α denotes the working angle of 15° for 24-sided polygon and τ indicates the maximum tilt angle between mirror and axis, controlled within $8''$. Thus, $u_5 = 0.0001''$.

Since these uncertainty components are uncorrelated with zero correlation coefficients, the combined standard uncertainty is:

$$u = \sqrt{u_1^2 + u_2^2 + u_3^2 + u_4^2 + u_5^2} \approx 0.23''. \quad (16)$$

Assuming normal distribution with $k_{95} = 2$, the expanded uncertainty is:

$$U = u \times k_{95} = 0.46''. \quad (17)$$

5. Conclusions

To ensure rotary table positioning accuracy, this paper proposes a fully online calibration-compensation method for rotary table positioning errors. Based on the principles of Fourier-method self-calibration and harmonic error compensation, and leveraging the low-latency, high-speed characteristics of hardware circuitry, a rotary table positioning error calibration-compensation system was developed. This system achieves online calibration and real-time compensation of rotary table positioning errors. Experimental results show that the rotary table's positioning error decreased from $[-150.0'', 137.9'']$ to $[-1.3'', 1.6'']$ after compensation, demonstrating that the proposed system effectively reduces positioning error and improves rotary table accuracy.

The proposed method imposes specific requirements on read head mounting positions; consequently, its effectiveness in enhancing the accuracy of existing rotary tables may not be significant. However, the developed system enables long-term online monitoring, calibration, and compensation of rotary table positioning accuracy, thereby improving the precision of compact or cost-sensitive rotary tables. Simultaneously, this method can provide reliable data support for spindle condition monitoring and fault inspection.

Acknowledgements

This work was financially supported by the project of the National Key R&D Program of China (2023YFF0615703), the National Natural Science Foundation of China (52175526), and the Zhejiang Provincial Natural Science Foundation (TGC24E050001).

Appendices

The CORDIC algorithm is fundamentally a numerical iterative approximation method. In practical circuits, its calculation accuracy is affected by iteration count n and data bit-width b , leading to computational errors. Limited iteration counts n introduce approximation error δ , while finite data bit-width b causes rounding error ε .

Based on the CORDIC computational principle, it can be inferred that the approximation error does not exceed the rotation angle in the final iteration. Thus, the maximum approximation error δ_{max} of the CORDIC algorithm can be expressed as:

$$\delta \arctan[2^{-(n-1)}]_{max} \quad (A.1)$$

Consequently, the maximum approximation error δ_{max} of the CORDIC algorithm can be regarded as a function of the iteration count n . It is evident that this function exhibits a monotonically decreasing trend within its domain and approaches 0 as $n \rightarrow +\infty$. The local curve of this function is shown in Fig. A.1.

During angle calculation using the CORDIC algorithm, since the computation is based on fixed-point arithmetic numerical iteration, its accuracy directly relates to the data bit-width b in the iterative process. The quantization error caused by finite precision in each iteration is termed rounding error ε . Influenced by iteration, ε accumulates as follows:

$$\varepsilon = e(n) + \sum_{j=1}^{n-1} B(j)e(j), \quad (A.2)$$

where, $e(n)$ is the round-off error vector generated in the n iteration, $\sum_{j=1}^{n-1} B(j)e(j)$ is the cumulative rounding error vector from previous $n - 1$ iterations, $B(j) = \prod_{i=j}^{n-1} \sqrt{1 + 2^{-2i}}$.

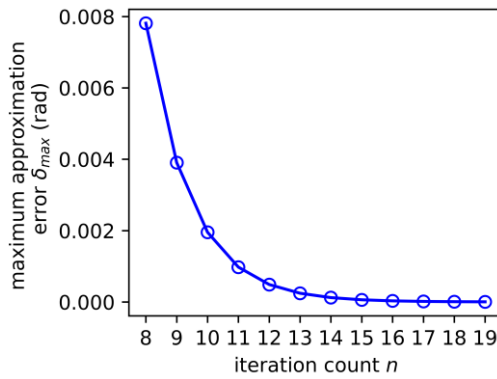


Fig. A.1. Schematic diagram of the maximum approximation error.

For the error vector $e(n) = [e_x(n) \quad e_y(n)]^T$:

$$\begin{cases} |e_x(n)| \leq 2^{-(b-1)} \\ |e_y(n)| \leq 2^{-(b-1)} \end{cases} \quad (A.3)$$

Thus, the bound of $|e(n)|$ is:

$$|e(n)| \leq \sqrt{e_x^2(n) + e_y^2(n)} \leq 2^{0.5-b}. \quad (A.4)$$

The maximum rounding error ε_{max} is:

$$\varepsilon_{max} = 2^{0.5-b} \left(1 + \sum_{j=1}^{n-1} \prod_{i=j}^{n-1} \sqrt{1 + 2^{-2i}} \right) \quad (A.5)$$

Consequently, the maximum rounding error ε_{max} is a function of iteration count n and data bit-width b . Its local curve is shown in Fig. A.2.

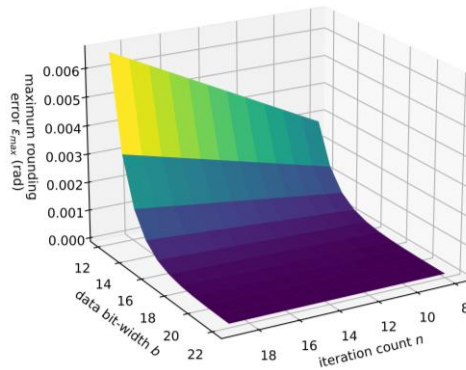


Fig. A. 2. Schematic diagram of the maximum rounding error

Considering the maximum allowable error for harmonic function computation, we set the iteration count $n = 16$ and the data bit-width $b = 18$.

References

- [1] International Organization for Standardization. (2012). ISO 230-1:2012 – Test code for machine tools — Part 1: Geometric accuracy of machines operating under no-load or quasi-static conditions. ISO.
- [2] Zou, W., Huang, Y., Lin, H., & Xue, Z. (2024). New application and research of ring laser gyroscope in the field of angle Metrology. *IEEE Transactions on Instrumentation and Measurement*, 73, 1–12. <https://doi.org/10.1109/tim.2024.3449940>
- [3] Lu, X., Graetz, R., Amin-Shahidi, D., & Smeds, K. (2010). On-axis self-calibration of angle encoders. *CIRP Annals*, 59(1), 529–534. <https://doi.org/10.1016/j.cirp.2010.03.127>
- [4] Lu, X., & Trumper, D. (2007). Self-Calibration of On-Axis rotary encoders. *CIRP Annals*, 56(1), 499–504. <https://doi.org/10.1016/j.cirp.2007.05.119>
- [5] Watanabe, T., Fujimoto, H., Nakayama, K., Masuda, T., & Kajitani, M. (2001). Automatic high-precision calibration system for angle encoder. *Proceedings of SPIE, the International Society for Optical Engineering/Proceedings of SPIE*, 4401, 267. <https://doi.org/10.1117/12.445630>
- [6] Watanabe, T., Samit, W., Vatcharanukul, K., Tonmueanwai, A., & Drijarkara, A. P. (2014). High resolution SelfA rotary table by the interpolation Signal calibration. *Key Engineering Materials*, 625, 53–59. <https://doi.org/10.4028/www.scientific.net/kem.625.53>
- [7] Ishii, N., Taniguchi, K., Yamazaki, K., & Aoyama, H. (2018). Development of super-accurate angular encoder system with multi-detecting heads using VEDA method. *Journal of Advanced Mechanical Design Systems and Manufacturing*, 12(5), JAMDSM0106. <https://doi.org/10.1299/jamdsm.2018jamdsm0106>
- [8] Geckeler, R. D., Fricke, A., & Elster, C. (2006). Calibration of angle encoders using transfer functions. *Measurement Science and Technology*, 17(10), 2811–2818. <https://doi.org/10.1088/0957-0233/17/10/036>
- [9] Geckeler, R. D., Link, A., Krause, M., & Elster, C. (2014). Capabilities and limitations of the self-calibration of angle encoders. *Measurement Science and Technology*, 25(5), 055003. <https://doi.org/10.1088/0957-0233/25/5/055003>
- [10] Hong-Sheng, W., Qi-Feng, Z., Dong, Q., & Bang-Hui, G. (2011). Filtering method of improving quality of grating Moiré fringe. *Optics and Precision Engineering*, 19(8), 1944–1949. <https://doi.org/10.3788/ope.20111908.1944>
- [11] Yang, R., Tan, K. K., Tay, A., Huang, S., Sun, J., Fuh, J., Wong, Y. S., Teo, C. S., & Wang, Z. (2016). An RBF neural network approach to geometric error compensation with displacement measurements only. *Neural Computing and Applications*, 28(6), 1235–1248. <https://doi.org/10.1007/s00521-016-2486-2>
- [12] Park, J. W., Nguyen, H. X., Tran, T. N., & Jeon, J. W. (2021). A linear compensation method for improving the accuracy of an absolute multipolar magnetic encoder. *IEEE Access*, 9, 19127–19138. <https://doi.org/10.1109/access.2021.3054362>

- [13] Zhao, C., Wan, Q., & Liang, L. (2024a). Automatic compensation system for eccentricity error of absolute optical encoder. *Review of Scientific Instruments*, 95(7). <https://doi.org/10.1063/5.0211297>
- [14] Zhao, G., Ban, Y., Zhang, Z., Wang, X., Chen, B., Shi, Y., Jiang, W., & Liu, H. (2024). Error compensation strategy with high installation tolerance for angle encoders. *Precision Engineering*, 91, 568–576. <https://doi.org/10.1016/j.precisioneng.2024.10.017>
- [15] Zhou, Y., Zhu, W., Shu, Y., Huang, Y., Zou, W., & Xue, Z. (2022). Analysis and application of real-time compensation of positioning precision of the turntable with a harmonic function. *Metrology and Measurement Systems*, 553–571. <https://doi.org/10.24425/mms.2022.142269>
- [16] Gurauskis, D., Kilikevičius, A., Borodinas, S., & Kasparaitis, A. (2019). Analysis of geometric and thermal errors of linear encoder for real-time compensation. *Sensors and Actuators a Physical*, 296, 145–154. <https://doi.org/10.1016/j.sna.2019.06.055>
- [17] Zhao, C., Wan, Q., & Liang, L. (2024b). Automatic compensation system for small absolute optical encoders. *IEEE Sensors Journal*, 24(19), 29778–29785. <https://doi.org/10.1109/jsen.2024.3442916>
- [18] Takahashi, N., Watanabe, T., & Tobita, K. (2025). SelfA-inclinometer: A novel device for evaluating the accuracy of tilting rotary tables in five-axis machine tools. *Precision Engineering*, 95, 38–51. <https://doi.org/10.1016/j.precisioneng.2025.04.009>
- [19] Huang, Y., Xue, Z., Qiao, D., Wang, Y., Yue, C., Liu, G., & Wang, Z. (2016). Study on the metrological performance of self-calibration angle encoder. *Proceedings of SPIE, the International Society for Optical Engineering/Proceedings of SPIE*, 9684, 96840O. <https://doi.org/10.1117/12.2246004>
- [20] Huang, Y., Xue, Z., Huang, M., & Qiao, D. (2018). The NIM continuous full circle angle standard. *Measurement Science and Technology*, 29(7), 074013. <https://doi.org/10.1088/1361-6501/aac6a6>
- [21] Kim, J., Kim, J. W., Kang, C., Jin, J., & Eom, T. B. (2013). Calibration of angle artifacts and instruments using a high precision angle generator. *International Journal of Precision Engineering and Manufacturing*, 14(3), 367–371. <https://doi.org/10.1007/s12541-013-0051-9>
- [22] Wang, Y., Xue, Z., Huang, Y., & Wang, X. (2016). Study on self-calibration angle encoder using simulation method. *Proceedings of SPIE, the International Society for Optical Engineering/Proceedings of SPIE*, 9903, 99032O. <https://doi.org/10.1117/12.2217638>
- [23] Zhao, J., Ou, W., Cai, N., Wu, Z., & Wang, H. (2024). Measurement Error Analysis and Compensation for Optical Encoders: A review. *IEEE Transactions on Instrumentation and Measurement*, 73, 1–30. <https://doi.org/10.1109/tim.2024.3417589>
- [24] Gao, W., Ibaraki, S., Donmez, M. A., Kono, D., Mayer, J., Chen, Y., Szpika, K., Archenti, A., Linares, J., & Suzuki, N. (2023). Machine tool calibration: Measurement, modeling, and compensation of machine tool errors. *International Journal of Machine Tools and Manufacture*, 187, 104017. <https://doi.org/10.1016/j.ijmachtools.2023.104017>
- [25] Shao, K., Zhu, W., Huang, Y., Xue, Z., Zhu, J., Kong, M., Zou, W., & Yin, Z. (2025). A study of the crucial parameters of Fourier method for improving the precision of rotary table. *Measurement*, 256, 118390. <https://doi.org/10.1016/j.measurement.2025.118390>
- [26] Andraka, R. (1998). A survey of CORDIC algorithms for FPGA based computers. In *Proceedings of the 1998 ACM/SIGDA Sixth International Symposium on Field Programmable Gate Arrays* (pp. 191–200). Association for Computing Machinery. <https://doi.org/10.1145/275107.275139>
- [27] AMD *zynq™ 7000 SoCs*. (n.d.). AMD. Retrieved 7 July 2025, from <https://www.amd.com/en/products/adaptive-socs-and-fpgas/soc/zynq-7000.html>
- [28] Li, G., He, Y., Gong, Z., Zhao, X., & Zhang, L. (2025). Deformation characteristics and angular error compensation of taper-mounted circular grating optical encoders. *Measurement*, 253, 117694. <https://doi.org/10.1016/j.measurement.2025.117694>



Kairu Shao received his B.Sc. degree from China Jiliang University in 2023. He is currently pursuing his master degree at China Jiliang University. His research interest is the angle measurement.



Yao Huang (Corresponding author) received his Ph.D. degree from Zhejiang University in 2025. He worked at the Geometric Lab of Beijing Metrology Institute from 2007 to 2013 and joined the Division of Metrology in Length and Precision Engineering of National Institute of Metrology in 2013. His main research interest is angle measurement.



Weibin Zhu (Corresponding author) received his Ph.D. degree in control theory and control engineering from Zhejiang University in 2014. He is currently a professor at China Jiliang University. His current interests include the grating signal processing and precision angle measurement.



Zi Xue received her Ph.D. degree from Harbin Technical University in 2006. She joined the Division of Metrology in Length and Precision Engineering of the National Institute of Metrology in 1991. Her main research interest is geometric measurement.



Jin Zhu received his M. Sc. degree from China Jiliang University in 2022, and is currently working at Zhejiang Institute of Quality Sciences. His main research interest is geometric measurement.